# A RESEARCH ON THE REVERSE TAPERING METHOD TO GAIN HIGH POWER POLARIZED PHOTON BEAM WITH FIXED WAVELENGTH

C. H. Shim, I. S. Ko, Pohang University of Science and Technology, Pohang 790-784, Korea

J. -H. Han, Y. W. Parc#, Pohang Accelerator Laboratory, Pohang 790-784, Korea

## Abstract

Polarization of soft X-ray photon can be controlled with combination between planar undulators and helical ones. We need to give a reverse tapering to the planar undulators to make microbunching in the electron beam while the linearly polarized radiation power is depressed. In this case, however, resonance wavelengths in each planar undulator are different each other. Therefore, proper initial undulator parameter and tapering strength parameter have to be chosen to obtain high power polarized photon beam with fixed wavelength. In this research, method for deciding suitable reverse tapering is presented using simulation results of PAL-XFEL soft X-ray case with 10 GeV electron beam energy.

# INTRODUCTION

In the soft X-ray regime, polarization control is essential for some experiments [1]. Applying the reverse tapering method to planar undulator section, the high degree of polarization of photon beam can be obtained by using only a couple of helical undulators, and this scheme is demonstrated at LCLS. [2,3].

Objective of undulator tapering is generally to obtain high radiation power by maintaining resonance condition according to decreasing electron beam energy [2]. In the reverse tapering case, however, resonance conditions in each planar undulator are different each other, so resonance wavelength is also changed along planar undulators. Therefore, appropriate initial undulator parameter and tapering strength parameter have to be selected to gain high power photon beam with fixed wavelength.

In this research, method for choosing suitable reverse tapering is presented using simulation results of PAL-XFEL soft X-ray case with 10 GeV electron beam energy. All simulations are performed as time-dependent model in GENESIS 1.3 using real beam properties [4].

# THEORY

## Reverse Tapering Method

In the reverse tapering method, undulator parameter $a_w$ is increased along the undulator length as shown in Fig. 1 [2]. Bunching factor is growing while radiation power is quite suppressed compared with non-tapering case. Tapering strength parameter, $\beta$, is defined as

$$\beta = -\frac{\lambda_u}{4\pi\rho^2}\frac{a_w(0)}{1+a_w(0)^2}\frac{da_w}{dz}$$

where $\lambda_u$ is period of undulator, $\rho$ is FEL parameter,
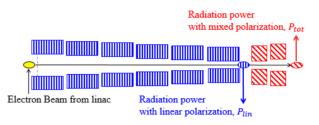
---

#young1@postech.ac.kr

Figure 1: Schematic diagram for reverse tapering method. (Blue Box) Reverse tapered planar undulators (Red Box) Helical undulators.

$a_w(0)$ is initial undulator parameter and $da_w/dz$ is derivative of undulator parameter along undulator length. When the reverse tapering method is applied, $\beta$ is negative.

## Polarization

Electric fields of linearly polarized radiation and circularly polarized radiation are given by the Eq. 1 [5].

$$\vec{E}_{lin} = E_{lin}\cos(kz - \omega t + \phi_{lin})\hat{x} \quad (1.a)$$

$$\vec{E}_{cir} = E_{cir}\cos(kz - \omega t + \phi_{cir})\hat{x}$$
$$+E_{cir}\cos(kz - \omega t \pm \pi/2 + \phi_{cir})\hat{y} \quad (1.b)$$

The circularly polarized radiation is amplified at the same phase of linearly polarized radiation, so $\phi_{lin}$ is equal to $\phi_{cir}$. Total electric field is given by the combination of two electric field equations and given by

$$\vec{E}_{tot} = \vec{E}_{lin} + \vec{E}_{cir}$$
$$= (E_{lin} + E_{cir})\cos(kz - \omega t + \phi_{cir} - \theta)\hat{x}$$
$$+E_{cir}\cos(kz - \omega t \pm \pi/2 + \phi_{cir})\hat{y} \quad (2)$$

The radiation power can be calculated from the electric field of radiation in Eq. 1 and Eq. 2 as follows [5]:

$$P_{lin} = E_{lin}^2 \quad (3.a)$$

$$P_{cir} = 2E_{cir}^2 \quad (3.b)$$

$$P_{tot} = (E_{lin} + E_{cir})^2 + E_{cir}^2 \quad (3.c)$$

In simulation, only $P_{lin}$ and $P_{tot}$ are obtained as shown in Fig. 1. So $P_{cir}$ is calculated using relations above and it is induced as follows:

$$P_{cir} = P_{tot} - \sqrt{P_{lin}(2P_{tot} - P_{lin})} \quad (4)$$

Stokes parameter is also expressed in terms of $P_{lin}$ and $P_{tot}$ as given by Eq. 5 [5].

$$S_0 = (E_{lin} + E_{cir})^2 + E_{cir}^2 = P_{tot} \quad (5.a)$$

$$S_1 = (E_{lin} + E_{cir})^2 - E_{cir}^2 = \sqrt{P_{lin}(2P_{tot} - P_{lin})} \quad (5.b)$$

$$S_2 = 2(E_{lin} + E_{cir})E_{cir}\cos(\pi/2) = 0 \quad (5.c)$$

$$S_3 = 2(E_{lin} + E_{cir})E_{cir}\sin(\pi/2) = P_{tot} - P_{lin} \quad (5.d)$$

The fraction of circularly polarized radiation, $|S_3/S_0|$, is given by Eq. 6 [6].

$$\left|\frac{S_3}{S_0}\right| = \frac{P_{cir} + \sqrt{2P_{lin}P_{cir}}}{P_{lin} + P_{cir} + \sqrt{2P_{lin}P_{cir}}} = 1 - \frac{P_{lin}}{P_{tot}} \quad (6)$$
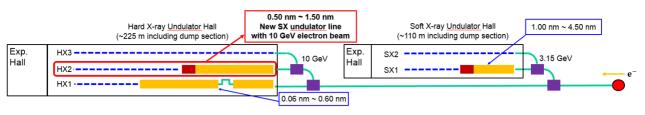
Figure 2: Schematic diagram about undulator lines of PAL-XFEL.

Using Eq. 6, the fraction of circularly polarized radiation is calculated using $P_{lin}$ and $P_{tot}$.

## PAL-XFEL SOFT X-RAY CASE

PAL-XFEL is 0.1 nm hard X-ray facility consisting of a 10 GeV S-band linac in Pohang, South Korea [7]. Installation of instruments is now in progress and the commissioning will start in 2016. There are one hard X-ray beamline with 10 GeV electron beam at the end of main linac and one soft X-ray beamline branch with 3.15 GeV electron beam in the middle part of the linac, as shown in Fig. 2.

New soft X-ray undulator line is proposed with 10 GeV electron beam for vacant wavelength region as highlighted by the red box in Fig. 2 [8]. Radiation performances are improved because of higher electron beam energy. In this simulation, new soft X-ray undulator line is used.

### 10 GeV Electron Beam

The 6-D particle distribution of electron beam is obtained by two tracking simulation tools (ASTRA for injector and ELEGANT for linac) [9,10]. Slice parameters of the electron beam for GENESIS 1.3 simulation are shown in Fig. 3. Bunch length is 18 μm and charge of electron beam is 180 pC. Electron beam current is slightly
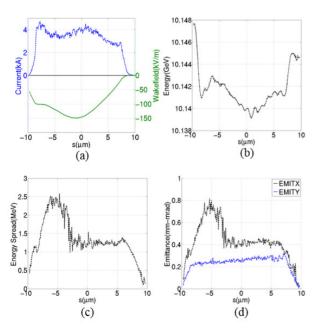


Figure 3: (a) Beam current (blue line) and wake field (green line). (b) Beam energy. (c) Energy spread. (d) Normalized emittance in x (black line) and y (blue line).
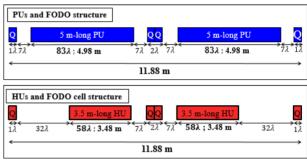


Figure 4: (top) FODO structure used in planar undulator section (bottom) FODO structure used in helical undulator section

higher than 3 kA as shown in Fig. 3 (a). Wakefield effect is calculated for flat beam pipe which has 8 mm inner height as shown by green line in Fig. 3 (a). Electron beam energy is about 10.14 GeV as shown in Fig. 3 (b). In Fig. 3 (c), the slice energy spread is little lower than 1.5 MeV except tail part, so relative energy spread is $1.48 \times 10^{-4}$. Normalized emittance in x and y direction is 0.4 mm-mrad and 0.2 mm-mrad as plotted in Fig. 3 (d), respectively.

### Undulator Lattice

FODO cell structures used for new soft X-ray undulator line in Fig. 2 are shown in Fig. 4 [8]. Every FODO structure is designed for using up to 5 m-long undulator. Undulator period, $\lambda_u$, is 60 mm in both planar and helical undulators. Length of planar and helical undulator is 5 m and 3.5 m, respectively. In the new undulator line, ten planar undulators and two helical undulators are used. Two helical undulators are located as near as possible for obtaining maximum radiation power from that [11].

## SIMULATION RESULTS

### Planar Undulator Section

In the vertical axis of Fig. 5, we need to show undulator parameter, $a_w$, for the first undulator module. However, to compare the first undulator's $a_w$ with the final radiation wavelength, we normalized $a_w$ as the same way to define the radiation wavelength with the resonance condition. We named the normalized $a_w$ as 'undulator's resonance wavelength' in this paper.

Reverse tapering method is applied to ten planar undulators and planar undulator's $a_w$ is increased linearly. Fixed (or desired) wavelength in this simulation is 1 nm. Final planar undulator's resonance wavelength is plotted in Fig. 5 (a) according to initial planar undulator's
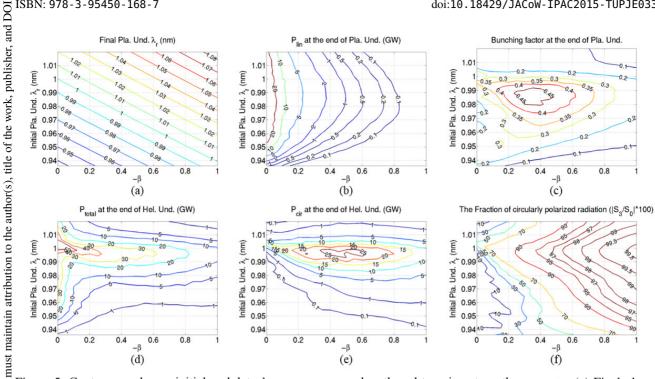
Figure 5: Contour graphs vs. initial undulator's resonance wavelength and tapering strength parameter (a) Final planar undulator's resonance wavelength (b) The power of linearly polarized radiation from planar undulator section (c) The bunching factor from planar undulator section (d) The total power of linearly and circularly polarized radiation from helical undulator section (e) The calculated power of circularly polarized radiation from helical undulator section (f) The fraction of circularly polarized radiation from helical undulator section.

resonance wavelength and tapering strength parameter, $\beta$.

The power of linearly polarized radiation after planar undulators, $P_{lin}$, is shown in Fig. 5 (b). The stronger $\beta$ is applied, the more $P_{lin}$ is depressed regardless of initial undulator's resonance wavelength.

Bunching factor of electron beam is shown in Fig. 5 (c) and values are decreasing slowly as $\beta$ is increasing. In the range of initial resonant wavelength from 0.98 nm to 0.99 nm and $\beta$ from 0.3 to 0.4, maximum bunching factor can be obtained.

*Helical Undulator Section*

Total power of linearly and circularly polarized radiation at the end of helical undulator, $P_{tot}$, is shown in Fig. 5 (d). Initial undulator's resonance wavelength has to be slightly shorter in all $\beta$ for obtaining maximized $P_{tot}$. $P_{tot}$ is decreased as $\beta$ is increased.

The power of circularly polarized radiation calculated by Eq. 4, $P_{cir}$, is plotted in Fig 5. (e). In the range of initial resonant wavelength from 0.995 nm to 0.999 nm and $\beta$ from 0.35 to 0.60, maximum $P_{cir}$ can be obtained. To gain high $P_{cir}$, initial undulator's resonance wavelength has to be slightly shorter than desired wavelength, same as $P_{tot}$. In spite of high $P_{tot}$ in low $\beta$ region, however, $P_{cir}$ is decreased as $\beta$ approaches zero because of high $P_{lin}$.

The fraction of circularly polarized radiation calculated by Eq. 6 is shown in Fig 5. (f). Initial undulator's resonance wavelength has to be slightly shorter in all $\beta$ for obtaining high fraction of circularly polarized radiation same as $P_{tot}$ and $P_{cir}$. The stronger $\beta$ is applied

to planar undulators, the higher fraction of circularly polarized radiation is obtained.

## CONCLUSION

Initial planar undulator's resonance wavelength has to be slightly shorter than fixed wavelength in all tapering strength parameter, $\beta$. Then maximum power of circularly polarized photon beam, $P_{cir}$, is gained in the appropriate range of $\beta$. The higher $\beta$ is applied to planar undulators, the higher fraction of circularly polarized radiation is obtained. However, $P_{cir}$ will be decreased after the appropriate range of $\beta$ mentioned above.

More simulation study will be conducted by changing the number of total planar undulators to understand the properties of reverse tapering method more clearly.

## REFERENCES

[1] S. Sasaki, Nucl. Instrum. Methods Phys. Res., Sect. A **347**, 83 (1994).

[2] E. A. Schneidmiller and M. V. Yurkov, Phys. Rev. ST AB **16**, 110702 (2013)

[3] J. MacArthur, A. Marinelli, A. Lutmann, T. Maxwell, H. –D. Nuhn, D. Ratner, Z. Huang, in *Proceedings of FEL2014* (Basel, Switzerland, 2014), TUP035.

[4] S. Reiche, Nucl. Inst. And Meth. A **429**, 243 (1999)

[5] E. Hecht, *Optics 4th* (Addison Wesley, New York, 2002).

[6] Y. Li, B. Faatz, J. Pflueger, E. L. Saldin, E. A. Schneidmiller, M. V. Yurkov, in *Proceedings of EPAC08* (Genoa, Italy, 2008), p. 2282.

[7]  I. S. Ko and J.-H. Han, "Current status of PAL-XFEL," in *Proceedings of the 27th Linear Accelerator Conference*, Geneva, Switzerland, MOIOB04 (2014)

[8]  To be presented at FEL2015

[9]  K. Flöttmann, ASTRA manual v3 (2011). http://www.desy.de/~mpyflo/Astra_dokumentation/

[10]  M. Borland, APS LS-287 (2000). http://www.aps.anl.gov/science/Publications/lsnotes/

[11]  C. H. Shim, I. S. Ko, Y. W. Parc and J.-H. Han, J. Korean Phys. Soc., submitted.